SCIENTIFIC REPORTS

OPEN

SUBJECT AREAS:
BIOANALYTICAL CHEMISTRY
OPTICAL IMAGING

Received
11 December 2013

Accepted
12 March 2014

Published
31 March 2014

Correspondence and requests for materials should be addressed to C.Z.H. (chengzhi@swu.edu.cn)

Real-Time Light Scattering Tracking of Gold Nanoparticles- bioconjugated Respiratory Syncytial Virus Infecting HEp-2 Cells

Xiao-Yan Wan[1], Lin-Ling Zheng[2], Peng-Fei Gao[1], Xiao-Xi Yang[1], Chun-Mei Li[1], Yuan Fang Li[2] & Cheng Zhi Huang[1,2]

[1]Key Laboratory of Luminescence and Real-Time Analytical Chemistry (Southwest University), Ministry of Education, College of Pharmaceutical Sciences, Southwest University, [2]College of Chemistry and Chemical Engineering, Southwest University, Chongqing 400715, China.

Real-time tracking of virus invasion is crucial for understanding viral infection mechanism, which, however, needs simple and efficient labeling chemistry with improved signal-to-noise ratio. For that purpose, herein we investigated the invasion dynamics of respiratory syncytial virus (RSV) through dark-field microscopic imaging (iDFM) technique by using Au nanoparticles (AuNPs) as light scattering labels. RSV, a ubiquitous, non-segmented, pleiomorphic and negative-sense RNA virus, is an important human pathogen in infants, the elderly, and the immunocompromised. In order to label the enveloped virus of paramyxoviridae family, an efficient streptavidin (SA)-biotin binding chemistry was employed, wherein AuNPs and RSV particles modified with SA and biotin, respectively, allowing the AuNP-modified RSVs to maintain their virulence without affecting the native activities of RSV, making the long dynamic visualization successful for the RSV infections into human epidermis larynx carcinoma cells.

Optical imaging has been widely used in biology and medicine[1–4], wherein traditional organic dyes and fluorescent proteins are commonly used as tags in bio-labeling because of their brightness over a short period[5,6]. However, the usefulness of these tags over comparative long periods is limited owing to their photobleaching properties and low emission efficiency. Quantum dots (QDs), although successfully applied in imaging owing to their bright emissions and possessed greater photostability than organic dyes[6–12], are easily aggregated and potential toxic[13–15]. Compared with other labeling materials, on the other hand, gold nanoparticles (AuNPs) appear to be superior as they have high levels of biocompatibility, unique optical properties for localized surface plasmon resonance (LSPR), and strong light scattering properties at their plasmon resonance frequency[16–19]. Therefore, it is crucial to choose the label materials so as to real-time visualize and track the dynamic processes, for example, how an individual virus particle infects cells[17,20–23]. Therefore, many researchers have adopted different labeling approaches, such as QDs label and immunofluorescent protein label, to study viral invasion[24–26], so that it is much better understanding the true mechanism(s) of virus invasion, which is crucial to prevention and control of viral diseases.

For real-time tracking of viral infection processes, it is basic to use fluorescence microscopy during the imaging process[21–23,27]. Compared to fluorescence microscopy imaging, dark-field microscopic imaging (*i*DFM) technique in which white light source was employed under a dark-field microscope to get scattering light signal, owing to metal nanoparticles of localized surface plasmon resonance[28], can resist photobleaching to keep signal intensity, so that the dark-field microscope which have been applied for long-time observing gets the images with high resolution and sensitivity. Based on this superiority, researchers have made significant contributions using *i*DFM technique for targeting cancer cells[19], intracellular imaging[29,30], drug release and photothermal therapy of cancer cells[31–34].

There have been few reports regarding real-time *i*DFM technique through light scattering to dynamically track the entrance of virus such as RSV into cells, human epidermis larynx carcinoma (HEp-2) cells, for example, to infect disease. Even if being too small to be observed, but if modified with AuNPs, the virus can be easily observed through the strong light scattering for a long time without affecting its native activities. RSV has a diameter ranging 150–300 nm, is a ubiquitous, non-segmented, pleiomorphic and negative-sense RNA virus, which is

crucial for the immunocompromised such as infants, and the elderly[35,36]. Our objectives were to efficiently label RSV with AuNPs, and conduct real-time imaging of RSV infecting HEp-2 cells. By using streptavidin (SA) modified AuNPs in this contribution, which could then have strong affinity to bind biotin-modified virus through biotin-NHS interactions with the amino groups on the viral surface, we could observe real time track single virus particles under a dark field microscope in the light scattering mode, and successfully monitor the viral infection over long periods.

Results

Features of the labeling chemistry. Fig. 1 shows our monitoring strategy for the viral invasion of cells, which generate AuNPs modified with SA. AuNPs were stable in solution because they were coated with a charged citrate layer on the surface. The citrate layer on the surface of AuNPs could be easily replaced in the presence of neutral or negatively charged SA in neutral medium, and the excessive active sites, which failed to be replaced on the surfaces, were blocked with further addition of bovine serum albumin (BSA).

The as-prepared AuNP-SA particles were centrifuged and suspended in phosphate-buffered saline (PBS). Then, the purified AuNP-SAs were used to label the RSV, which had been previously modified with biotin-NHS through interactions between the amino groups on the surface of RSV and biotin-NHS (Fig. 1). Owing to the strong light scattering of localized surface plasmon resonance (LSPR) resulted at the plasmon resonance frequency, the RSV labeled with AuNP (AuNP-RSV) could be clearly observed under a dark-field microscope.

Fig. 2 shows the optical features of different size of AuNPs with modifications with SA suspensions. It can be seen that the modifications of AuNPs, which have maximum absorption at 522, 518, 524, and 528 nm for AuNPs of 6.5, 13, 30, and 50 nm, respectively, have slight red shift owing to the attachment of SA and BSA onto the AuNP surface. The zeta potential of AuNPs was altered when their surfaces were modified (Fig. 3a), and viability assay of cells showed that the different size of AuNP-SAs had no obvious toxicity to cell growth and proliferation (Fig. 3b). These results showed that the various proteins were successfully bound to the surface of AuNPs. And AuNPs modified with SA and BSA did not show aggregation tendency to be stable in PBS buffer and had good biocompatibility.

Features of AuNP-labeled RSVs. Transmission electron microscopy (TEM) Images (Fig. 4) clearly showed the different characteristic features of both unlabeled and AuNP-labeled RSVs. The unmodified virus had a smooth membrane surface (Fig. 4a, appeared to be round or kidney shaped, with a diameter of about 200 nm, while the 13-nm AuNP-RSVs contained some AuNPs at the edge of the viral membrane, and on their surface (Fig. 4b). The 30-nm AuNP-RSVs, however, had less AuNPs attached compared with the 13-nm AuNP-RSVs. Further experiments illustrated that AuNPs with a smaller size had a greater propensity for labeling RSV, which might be because of the lower steric hindrance. In addition, the 13-nm AuNP-RSVs displayed better light scattering than the 30-nm AuNP-RSVs, which made us chose the 13-nm AuNP-RSVs for our real-time imaging experiments.

In order to find whether our labeling has effect on the virus, we measured the titers of viruses, which were expressed as the 50% tissue culture infectious dose ($TCID_{50}$) (Fig. 5) and the investigation of syncytium formation (Supplementary Fig. S1). The titers of RSV, biotin-RSV, and RSV labeled with AuNPs (AuNP-RSVs) of 6.5, 13, 30, and 50 nm were 2.6×10^7, 1.4×10^6, 1.0×10^6, 7.6×10^5, 6.6×10^5, and 2.5×10^5 $TCID_{50}$/mL, respectively, showed that labeling with AuNPs can scarcely exert influence on viral infectivity. After the HEp-2 cells were infected by RSV and biotin-RSV, respectively, and had been cultured for 24 h, the syncytium formed and could be easily observed (Supplementary Fig. S1). This result showed our labeling without effect on viral infectivity again. Moreover, with respect to the effects of AuNP size on RSV virulence, we found that $TCID_{50}$ values were similar except in the case of 50 nm AuNPs; Thence small size AuNPs were ideal labeling materials for our experiments.

Invasion of RSV labeled with AuNPs into host cells. Fig. 6 showed the results of the invasion of RSV labeled with AuNPs into HEp-2

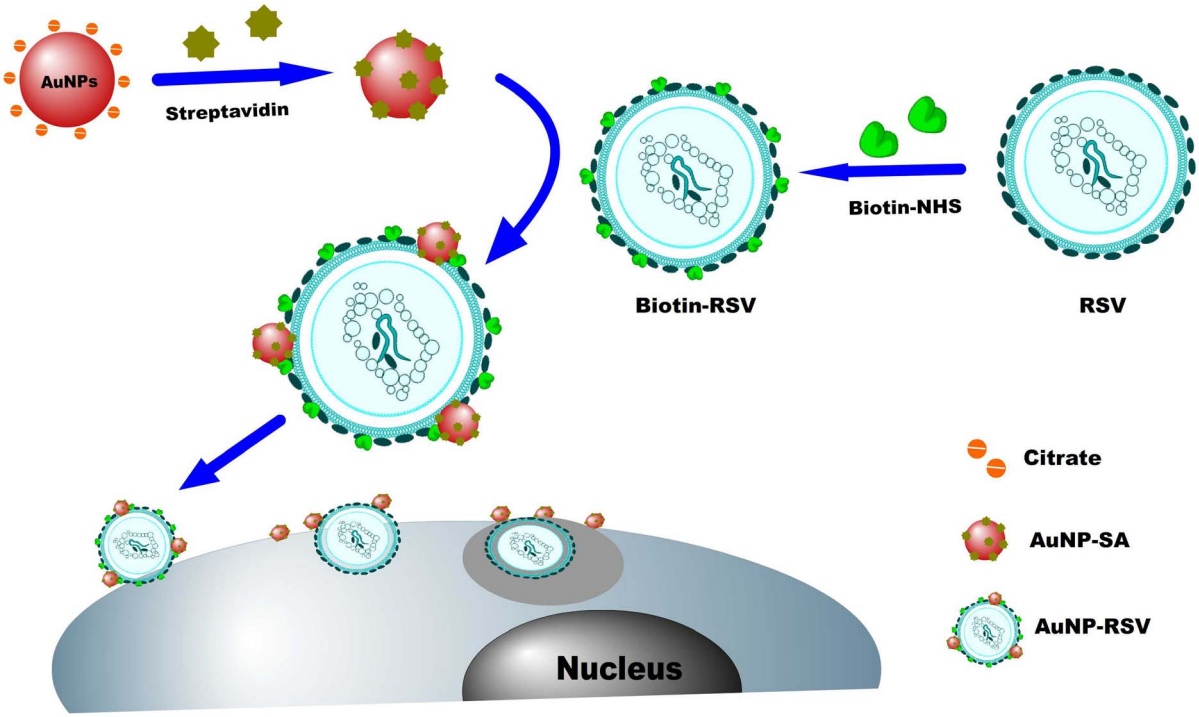

Figure 1 | Schematic outlining the generation of AuNPs conjugated with SA and RSV labeled with AuNP-SAs, then AuNP-RSVs invaded HEp-2 cells.

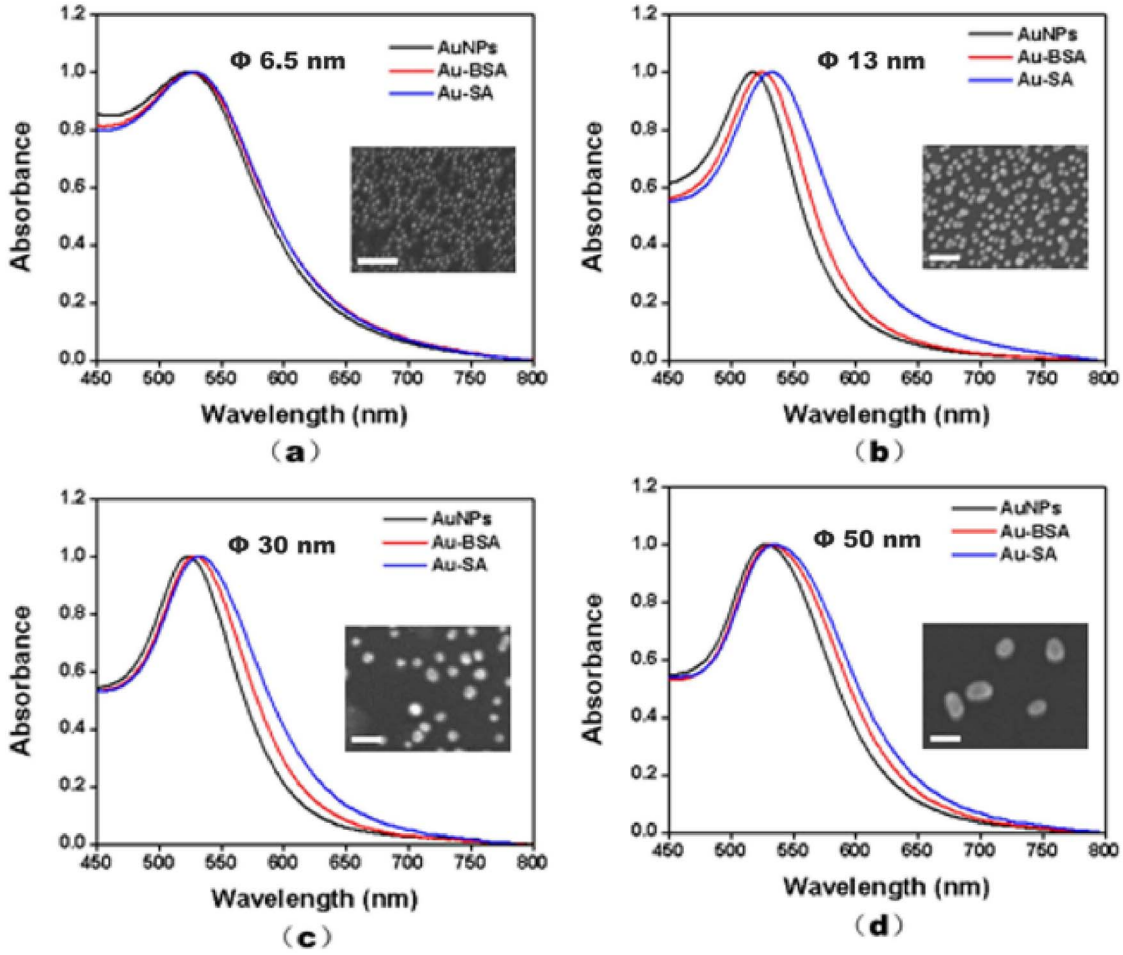

Figure 2 | **UV-vis absorption spectra of AuNPs (black line), Au-BSA (red line) and Au-SA (blue line).** The insets are the SEM images of AuNPs either modified or non-modified. The scale bars indicate 50 nm.

host cells. Owing to the light scattering of the cellular medium and the reflection light beam, the internals and outline of the HEp-2 cells could be observed under the DFM in light scattering mode (Fig. 6a). As it can be seen, the unmodified AuNPs can scarcely be non-specifically adsorbed on the cellular membrane (Fig. 6b), but the AuNPs modified with proteins can not be non-specifically absorbed completely (Fig. 6c and 6d). In other word, the active sites on the surface of AuNPs could be successfully blocked by using BSA. Fig. 6e showed that the HEp-2 cells could be easily observed for the AuNPs-modified RSV has been adsorbed on the cell surface, wherein AuNPs-modified RSV has strong light scattering signals owing to the localized surface plasmon resonance (LSPR) (Fig. 6e). That is to say, AuNP-RSV was able to attach to the cellular membrane by binding to the appropriate receptor on the

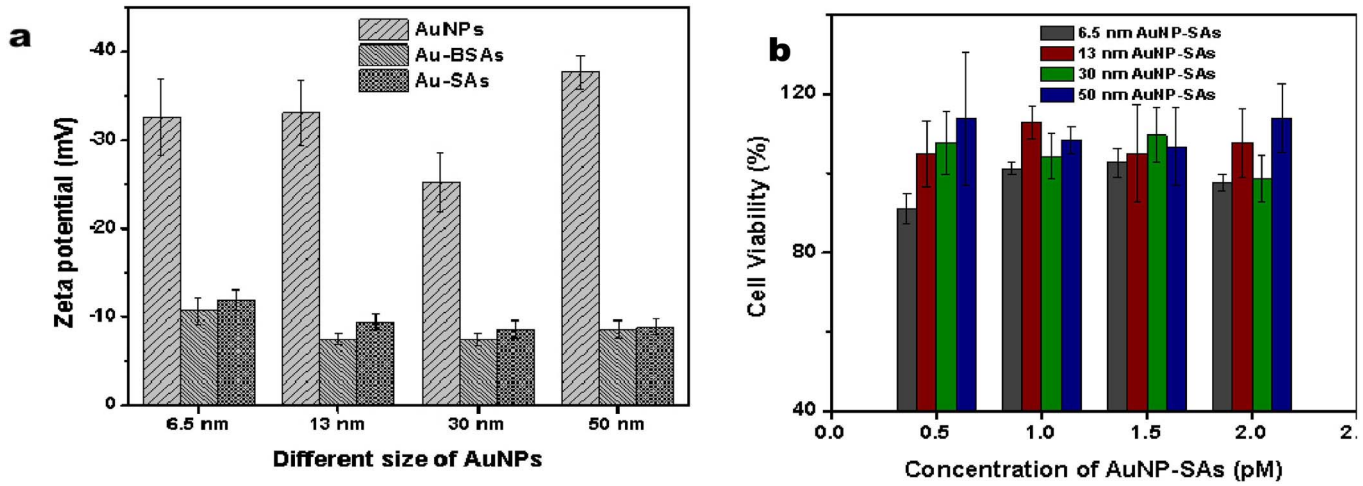

Figure 3 | **Characterization of AuNP-SAs.** (a) Zeta potential of AuNPs, AuNP-BSAs and AuNP-SAs used in our experiments. (b) CCK-8 detection of the viability of HEp-2 cells incubated with 6.5, 13, 30 and 50 nm AuNP-SAs at different concentrations for 24 h. Error bars represented the standard deviation from three replicated experiments.

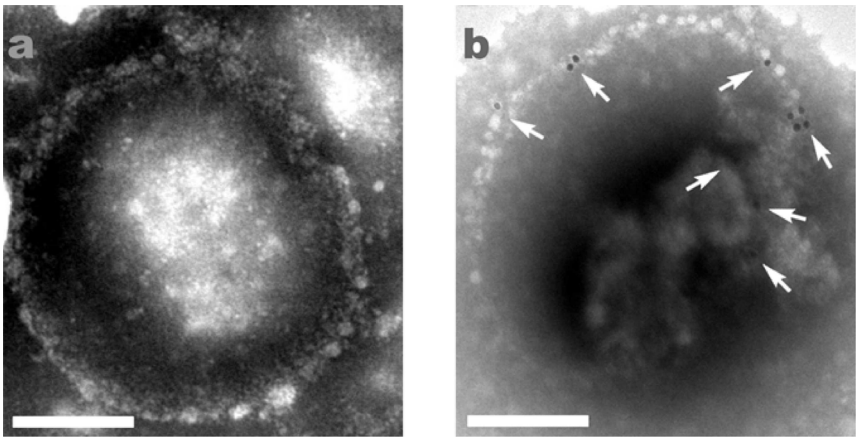

Figure 4 | TEM images of RSV (a) and RSV labeled with 13-nm AuNPs (b). The white arrows indicate the 13-nm AuNP-RSVs. The scale bars indicate 100 nm.

surface of the cell. In order to further identify the authenticity of result, we prepared QDs-labeled RSV by conjugating streptavidinylated quantum dots with biotin-RSV, and used it to image the infection process by fluorescence microscope (Supplementary Fig. S2). Furthermore, the immunofluorescence images of AuNP-RSVs and RSVs infecting cells at various post-infection time had been acquired (Supplementary Fig. S3). The results showed that the QDs-labeled RSV and AuNP-labeled RSV had the same infection routes with non-labeled RSV, indicating that the AuNP labeling had no obvious effect on RSV infection. In such case, Fig. 6e further indicated that the location of AuNPs on the cell membrane represented the location of viruses invading cells. The results and trends for AuNPs of different size were consistent (Fig. 6). Compared with AuNPs of a larger size, the light scattering of AuNPs with a diameter of 6.5 nm was weak. The results indicated that the size of AuNPs and the effects of AuNP size on RSV virulence should be considered when using iDFM technique in light scattering mode to monitor viruses infecting cells (Fig. 5 and Fig. 6). That means, AuNP-viruses with diameters of 13 and 30 nm were appropriate for dark-field imaging.

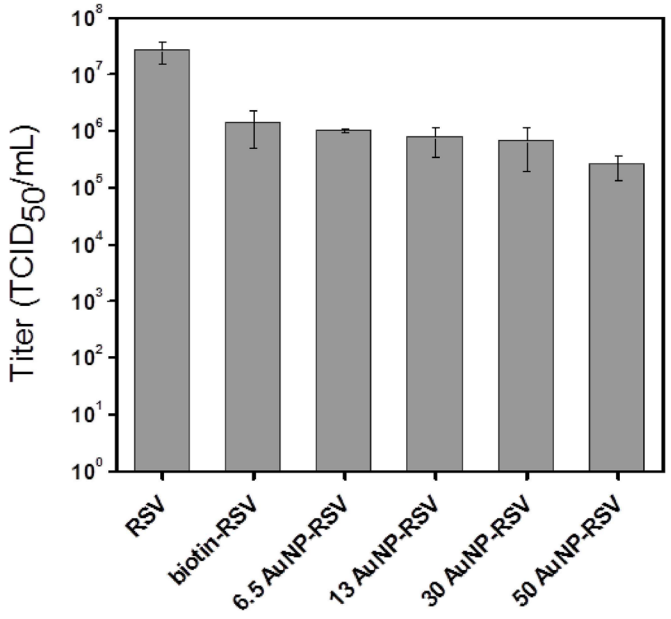

Figure 5 | Titers of the various virus conjugates with different size of AuNPs. 96-well plates were used to culture HEp-2 cells. Then the AuNP-RSVs solution with serially diluted by RPMI 1640 culture medium were added to the cells and infected for 2 h at 37°C. The infected cells in 96-well plates were cultured about 7 days. $TCID_{50}$ was calculated to quantify the titer of RSV.

Real-time dark-field light scattering imaging. The 13-nm AuNP-RSVs were used for real-time imaging, with those particles scattering orange light. The 30-nm AuNP-RSVs scattered light to a much less extent than that with the 13-nm particles, illustrating that smaller AuNPs were more likely to bind to RSV (Figure 5). In such case, the 13-nm AuNP-RSVs were successfully used to achieve superior real-time imaging results. As the movie (supplementary movie A) showed, the virus rapidly invaded the cellular membrane (red arrow) when the 13-nm AuNP-RSV solution was added (Fig. 7), indicating that RSV quickly invades host cells. Some AuNP-RSVs linked on the cell membrane when presented for a short time, and with increase of the time (100 s, for instance), they moved across the cell membrane. The entire invasion processes for the 13-nm AuNP-RSVs was between 1–2 min. During the invading process, the number of viral particles that moved across HEp-2 cells also increased (supplementary movie B), further illustrating that RSV labeled with 13-nm AuNPs were ideal because of the relatively low levels of steric hindrance. The real-time imaging of RSV infecting live cells can be achieved by monitoring the scattering light of AuNPs bound to the virus.

Discussion

AuNPs of different size were used to label RSV to facilitate real-time imaging of viral infection, displaying that AuNPs with the diameter of 13 nm could be successfully applied for the virus labeling in order to observe their invasion into cells. That means the invasion of a cell by viruses can be successfully monitored by measuring the scattered light from the AuNPs under a dark-field light scattering microscopy. The labeling strategy was simple and highly efficient, and the use of AuNPs as labels did not appear to adversely affect the infectivity of RSV, indicating that AuNPs with the size of 13 nm are a superior alternative for tracking viral infection without any obvious damage to cells even if real-time imaging conducted for long periods.

Methods

Materials and reagents. Respiratory syncytial virus (RSV) strain and human epidermis larynx carcinoma cell lines (HEp-2 cells) were cultivated and obtained in our own laboratory. Streptavidin (SA) was purchased from Beijing Boisynthesis Biotechnology Co. Ltd. (Beijing, China). Bovine serum albumin (BSA) was purchased from Beijing Dingguo Changsheng Biotechnology Co. Ltd. (Beijing, China). Biotin was purchased from Thermo (U.S.A). Streptavidin−quantum dot (QD) conjugates were purchased from Jiayuan Quantum Dot Co. Ltd. (Wuhan, China). Other commercial reagents such as $HAuCl_4$ and trisodium citrate were analytical reagent grade without further purification. All the above reagents were prepared with Milli-Q purified water (18.2 MΩ).

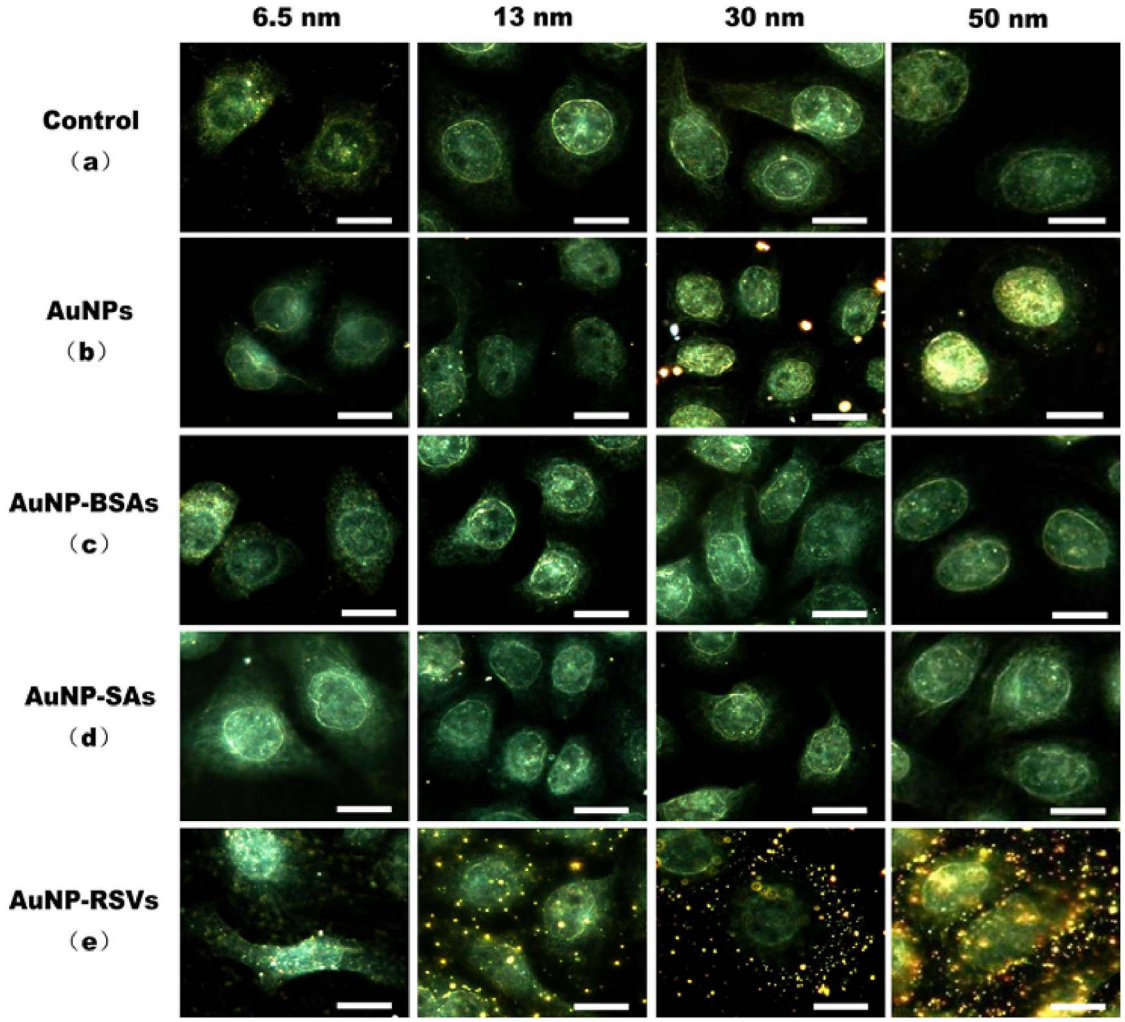

Figure 6 | Dark-field light scattering images acquired during viral infection. The control group is represented by HEp-2 cells (a). HEp-2 cells were incubated with AuNPs (b), AuNP-BSAs (c), AuNP-SAs (d) and AuNP-RSVs (e). The scale bars indicate 20 μm.

Preparation of AuNPs. The preparation of 13 nm Au Nanoparticles (AuNPs) was performed according to the well-established method for AuNPs synthesis[37]. 2 mL $HAuCl_4$ (1%, *w*/*w*) and 50 ml H_2O were added in a clean flask. Heat up the solution with magnetic stirring and add 1 mL 5% sodium citrate to the solution quickly when boiling. Allow the system to reflux for 5 min, then stop heating and continue stirring until cooling to room temperature. AuNPs were filtered by 0.22 μm membrane and stored in 4°C fridge. Monodispersed AuNPs of varying sizes, including 6.5, 13, 30 and 50 nm, were prepared by altering the quantity of $HAuCl_4$ and reducing agents (see Supplementary Methods).

Conjugation and characterization of AuNP-SAs. AuNPs conjugated with SA (AuNP-SAs) were prepared by incubating the as-prepared AuNPs with different sizes of 6.5, 13, 30 and 50 nm with SA (the corresponding concentration was 32, 80, 30 and 100 $\mu g \cdot L^{-1}$) for about 30 min at room temperature. The concentrations of the AuNPs were calculated to be 5.24×10^{-8}, 6.94×10^{-9}, 1.32×10^{-10} and 2.69×10^{-11} M. After that, BSA was used further to react for 30 min in order to block the excessive binding sites on AuNPs surface after the incubating reaction. The concentration of BSA was 64, 100, 80 and 350 $\mu g \cdot L^{-1}$, respectively. Spectroscopic properties and hydrodynamic diameter of AuNPs, AuNP-BSAs and AuNP-SAs were measured with a U-3010 spectrophotometer (Hitachi, Tokyo, Japan) and a Zetasizer Nano ZS90 (Malvern Instruments), respectively.

Cell culture and cells viability assay. The 2×10^5 cells$\cdot mL^{-1}$ HEp-2 cells in RPMI 1640 culture medium containing 10% (w/v) fetal bovine serum (FBS) were first added to each well of a 96-well plate (100 μL per well), and cultured at 37°C with 5% CO_2 for 24 h to make cells adhere to the surface. For another 24 h the culture medium was replaced with 100 μL of RPMI 1640 (2% FBS) containing different amounts of bulk 6.5, 13, 30 and 50 nm AuNP-SAs, respectively. Then, cells were incubated with the CCK-8 solution for 30 min after 96-well plate have been washed with PBS. The absorbance (450 nm) for each well was measured with a Microplate Reader Modle. Cell viability was determined by comparing the ratio of absorbance of the cells incubated with AuNP-SAs to that of the cells incubated with culture medium only.

Virus propagation. RSV was propagated in monolayer culture of HEp-2 cells at 37°C with 5% CO_2 in RPMI 1640 culture medium (2% FBS). At 1–2 days post infection, when the cytopathic effect (CPE) could be observed, the cell were subjected to 2–3 rounds of freeze-thaw cycles to release viruses and cell debris were removed by centrifugation at 3000 g for 10 min. The harvest RSV was stored at −80°C.

Virus titer assays. 50% tissue culture infective dose ($TCID_{50}$) was used to quantify the titer of RSV. 96-well plates were used to culture HEp-2 cells in culture medium for about 24 h at 37°C with 5% CO_2. Then the AuNP-RSVs solution with serially diluted by RPMI 1640 culture medium were added to the cells and infected for 2 h at 37°C. The infected cells in 96-well plates were cultured in RPMI 1640 culture medium supplemented with 2% FBS at 37°C with 5% CO_2 for about 7 days. Then $TCID_{50}$ was calculated according to the Reed-Muench formula: $TCID_{50}$ = dilution above 50% CPE + [(% next above 50%) − 50%]/(% next above 50% − (% next below 50%)) × log10.

Label of virus with AuNPs. RSV biotinylation was carried out by incubating viral suspension and biotin of 1 $mg \cdot mL^{-1}$ for about 2 h at 4°C, and then excessive biotin was removed by a desalting NAP-5 column (GE Healthcare). The AuNP-SAs and biotin-virus were mixed and reacted for about 10 min at 4°C. The control virus and AuNP-RSVs were characterized with TEM (JEM 1200EX, Japan Electronics Co. Ltd.) in terms of their size, morphology and labeling decorated situation by dropping the virus or AuNP-RSV onto the copper grid and negatively staining.

Dark-field light scattering imaging. HEp-2 cells were cultured on 12-well plates of coverslip for about 24 h in an incubator to reach 50% confluence before infection. Then 100 μL biotinylated viruses and 100 μL PBS buffer were successively added to 12-well plates and incubated for 20 min at 4°C, spare virus solution was removed and cells in 12-well plates were rinsed. 400 μL AuNP-SAs with 1.5 pM for 6.5 nm, or 1.5 pM for 13 nm, or 2.0 pM for 30 nm, or 2.0 pM for 50 nm were added and incubated for 30 min at 4°C. Then cells were fixed with 4% paraformaldehyde, sealed with glycerin, and then transferred for dark-field light scattering imaging under an

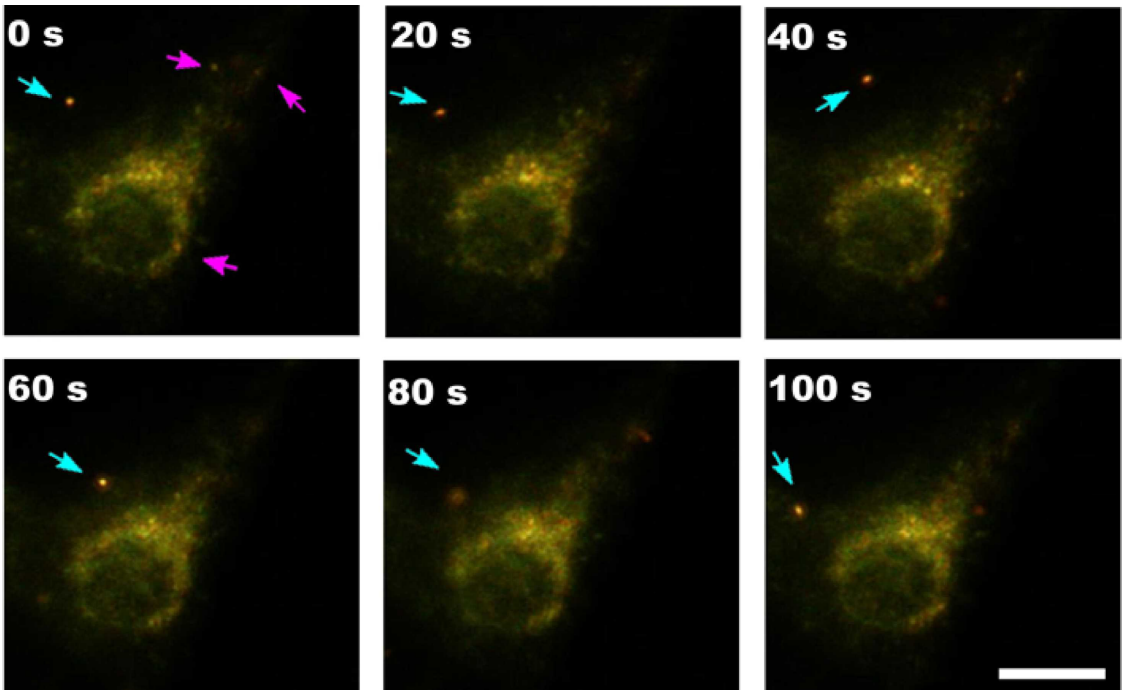

Figure 7 | Real-time dark-field light scattering images of 13-nm AuNP-RSVs invading HEp-2 cells. The red arrow indicates a virus on the cell membrane when the 13-nm AuNP-RSVs are added to living HEp-2 cells. The blue arrow indicates the infection process for a single AuNP-RSV invading HEp-2 cells, which occurs over 1 min following the addition of AuNP-RSV. The scale bar indicates 20 μm.

Olympus BX-51 microscope (Tokyo, Japan) with a 40× objective, which was equipped with a highly numerical dark field condenser (U-DCW). The colorful dark-field light scattering photographs of the AuNPs labeling virus were captured with an Olympus E-510 digital camera (Tokyo, Japan).

Real-time imaging of AuNP-RSVs infection cells. HEp-2 cells were cultured on a home-made plate for about 36 h at 37°C with 5% CO_2. AuNP-RSVs were added to cells and achieved real-time dark-field imaging of virus infecting cells for 20 min at the room temperature. This process was acquired with a dark-field microscope (Tokyo, Japan) with a 40× objective in a polarized light of ND6.

1. Li, C. *et al.* In vivo real-time visualization of tissue blood flow and angiogenesis using Ag2S quantum dots in the NIR-II window. *Biomaterials* **35**, 393–400 (2014).
2. Chen, G. *et al.* Tracking of Transplanted Human Mesenchymal Stem Cells in Living Mice using Near-Infrared Ag2S Quantum Dots. *Adv. Funct. Mater.* DOI: 10.1002/adfm.201303263 (2013).
3. Welsher, K. *et al.* A route to brightly fluorescent carbon nanotubes for near-infrared imaging in mice. *Nat. Nanotechnol.* **4**, 773–780 (2009).
4. Zhang, Y. *et al.* Ag2S Quantum Dot: A Bright and Biocompatible Fluorescent Nanoprobe in the Second Near-Infrared Window. *ACS Nano* **6**, 3695–3702 (2012).
5. Joo, K.-I. *et al.* Enhanced Real-Time Monitoring of Adeno-Associated Virus Trafficking by Virus–Quantum Dot Conjugates. *ACS Nano.* **5**, 3523–3535 (2011).
6. Hu, P. P. *et al.* Ultra-sensitive detection of prion protein with a long range resonance energy transfer strategy. *Chem. Commun.* **46**, 8285–8287 (2010).
7. Jin, Y. & Gao, X. Plasmonic fluorescent quantum dots. *Nat. Nanotechnol.* **4**, 571–576 (2009).
8. Choi, Y. *et al.* Intracellular Protein Target Detection by Quantum Dots Optimized for Live Cell Imaging. *Bioconjugate Chem.* **22**, 1576–1586 (2011).
9. Hao, J., Huang, L.-L., Zhang, R., Wang, H.-Z. & Xie, H.-Y. A Mild and Reliable Method to Label Enveloped Virus with Quantum Dots by Copper-Free Click Chemistry. *Anal. Chem.* **84**, 8364–8370 (2012).
10. Du, Y. *et al.* Near-Infrared Photoluminescent Ag2S Quantum Dots from a Single Source Precursor. *J. Am. Chem. Soc.* **132**, 1470–1471 (2010).
11. Welsher, K., Sherlock, S. P. & Dai, H. Deep-tissue anatomical imaging of mice using carbon nanotube fluorophores in the second near-infrared window. *Proc. Natl. Sci.* **108**, 8943–8948 (2011).
12. Hong, G. *et al.* In Vivo Fluorescence Imaging with Ag2S Quantum Dots in the Second Near-Infrared Region. *Angew. Chem. Int. Ed.* **51**, 9818–9821 (2012).
13. Ropp, C. *et al.* Nanoscale imaging and spontaneous emission control with a single nano-positioned quantum dot. *Nat. Commun.* **4**, 1447 (2013).
14. Lodahl, P. *et al.* Controlling the dynamics of spontaneous emission from quantum dots by photonic crystals. *Nature* **430**, 654–657 (2004).
15. Auffan, M. *et al.* Towards a definition of inorganic nanoparticles from an environmental, health and safety perspective. *Nat. Nanotechnol.* **4**, 634–641 (2009).
16. Jayagopal, A., Halfpenny, K. C., Perez, J. W. & Wright, D. W. Hairpin DNA-Functionalized Gold Colloids for the Imaging of mRNA in Live Cells. *J. Am. Chem. Soc.* **132**, 9789–9796 (2010).
17. Everts, M. *et al.* Covalently Linked Au Nanoparticles to a Viral Vector: Potential for Combined Photothermal and Gene Cancer Therapy. *Nano Lett.* **6**, 587–591 (2006).
18. Huang, Y.-F., Lin, Y.-W., Lin, Z.-H. & Chang, H.-T. Aptamer-modified gold nanoparticles for targeting breast cancer cells through light scattering. *J Nanopart Res* **11**, 775–783 (2009).
19. Popovtzer, R. *et al.* Targeted Gold Nanoparticles Enable Molecular CT Imaging of Cancer. *Nano Lett.* **8**, 4593–4596 (2008).
20. Chen, L. Q. *et al.* Aptamer-Based Silver Nanoparticles Used for Intracellular Protein Imaging and Single Nanoparticle Spectral Analysis. *J. Phys. Chem. B* **114**, 3655–3659 (2010).
21. Joo, K.-I. *et al.* Site-Specific Labeling of Enveloped Viruses with Quantum Dots for Single Virus Tracking. *ACS Nano.* **2**, 1553–1562 (2008).
22. Zhang, P. *et al.* Click-Functionalized Compact Quantum Dots Protected by Multidentate-Imidazole Ligands: Conjugation-Ready Nanotags for Living-Virus Labeling and Imaging. *J. Am. Chem. Soc.* **134**, 8388–8391 (2012).
23. Huang, B.-H. *et al.* Surface Labeling of Enveloped Viruses Assisted by Host Cells. *ACS Chem. Biol.* **7**, 683–688 (2012).
24. van der Schaar, H. M. *et al.* Dissecting the cell entry pathway of dengue virus by single-particle tracking in living cells. *PLoS pathogens* **4**, e1000244 (2008).
25. Liu, H., Liu, Y., Liu, S., Pang, D. W. & Xiao, G. Clathrin-mediated endocytosis in living host cells visualized through quantum dot labeling of infectious hematopoietic necrosis virus. *J. Virol.* **85**, 6252–6262 (2011).
26. McDonald, D. *et al.* Visualization of the intracellular behavior of HIV in living cells. *J Cell Biol.* **159**, 441–452 (2002).
27. Huang, L.-L. *et al.* Enveloped Virus Labeling via Both Intrinsic Biosynthesis and Metabolic Incorporation of Phospholipids in Host Cells. *Anal. Chem.* **85**, 5263–5270 (2013).
28. Hu, M. *et al.* Dark-field microscopy studies of single metal nanoparticles: understanding the factors that influence the linewidth of the localized surface plasmon resonance. *J. Mater. Chem.* **18**, 1949–1960 (2008).
29. Kang, B., Mackey, M. A. & El-Sayed, M. A. Nuclear Targeting of Gold Nanoparticles in Cancer Cells Induces DNA Damage, Causing Cytokinesis Arrest and Apoptosis. *J. Am. Chem. Soc.* **132**, 1517–1519 (2010).
30. Zhang, L. *et al.* Single Gold Nanoparticles as Real-Time Optical Probes for the Detection of NADH-Dependent Intracellular Metabolic Enzymatic Pathways. *Angew. Chem. Int. Ed.* **50**, 6789–6792 (2011).
31. Ungureanu, C. *et al.* Light Interactions with Gold Nanorods and Cells: Implications for Photothermal Nanotherapeutics. *Nano Lett.* **11**, 1887–1894 (2011).

32. Jain, P. K., Huang, X., El-Sayed, I. H. & El-Sayed, M. A. Noble Metals on the Nanoscale: Optical and Photothermal Properties and Some Applications in Imaging, Sensing, Biology, and Medicine. *Acc. Chem. Res.* **41**, 1578–1586 (2008).
33. Lee, M.-Y. *et al.* Hyaluronic Acid–Gold Nanoparticle/Interferon α Complex for Targeted Treatment of Hepatitis C Virus Infection. *ACS Nano.* **6**, 9522–9531 (2012).
34. Huang, X., El-Sayed, I. H., Qian, W. & El-Sayed, M. A. Cancer Cell Imaging and Photothermal Therapy in the Near-Infrared Region by Using Gold Nanorods. *J. Am. Chem. Soc.* **128**, 2115–2120 (2006).
35. Brown, G. *et al.* Analysis of the interaction between respiratory syncytial virus and lipid-rafts in Hep2 cells during infection. *j.virol.* **327**, 175–185 (2004).
36. Melero, J. A. in *J.A. Melero* Vol. Volume 14 (ed Cane, Patricia) 1–42 (Elsevier, 2006).
37. Zou, B. Z., Liu, Y., Yan, X. L. & Huang, C. Z. Gold nanoparticles based digital color analysis for quinidine detection. *Chin Sci Bull* **58**, 2027–2031 (2013).

Acknowledgments

This work was supported by the Ministry of Science and Technology of the People's Republic of China (Grant 2011CB933600) and the Cultivation Plan of Chongqing Science & Technology Commission for 100 Outstanding Science and Technology Leading Talents.

Author contributions

Experiments were designed by C.Z.H. and X.Y.W. Material characterizations were carried out by X.Y.W. Computer simulation was done by X.Y.W. and P.F.G. Cell Culture and Virus Propagation were performed by X.Y.W., X.X.Y. and C.M.L. Real-time dark-field imaging was performed by X.Y.W. and L.L.Z. The manuscript was written by C.Z.H., Y.F.L. and X.Y.W.

Additional information

Supplementary information accompanies this paper at http://www.nature.com/scientificreports

Competing financial interests: The authors declare no competing financial interests.

How to cite this article: Wan, X.-Y. *et al.* Real-Time Light Scattering Tracking of Gold Nanoparticles- bioconjugated Respiratory Syncytial Virus Infecting HEp-2 Cells. *Sci. Rep.* **4**, 4529; DOI:10.1038/srep04529 (2014).